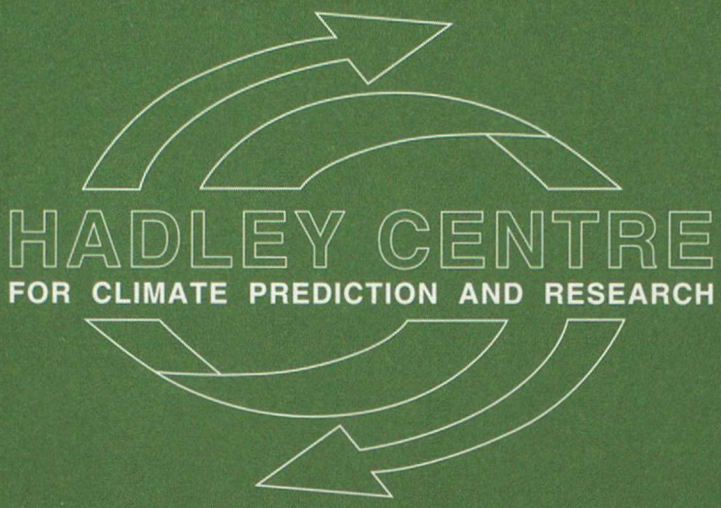

North Atlantic and European seasonal predicability using an ensemble of multi-decadal AGCM simulations

by

J R Davies, D P Rowell and C K Folland

CRTN 70

May 1996

CLIMATE
RESEARCH
TECHNICAL
NOTE

Hadley Centre
Meteorological Office
London Road
Bracknell
Berkshire RG12 2SY

North Atlantic and European Seasonal Predictability using an Ensemble of Multi-Decadal AGCM Simulations

John R. Davies, David P. Rowell* and Chris K. Folland

* Corresponding author

Hadley Centre for Climate Prediction and Research,
Meteorological Office, London Road,
Bracknell, Berkshire, RG12 2SY, U.K.

Tel: 01344-856077
Fax: 01344-854898
E-mail: dprowell@meto.govt.uk

Manuscript submitted May 1996

ABSTRACT

An initial study of seasonal predictability for the North Atlantic and European regions is presented, using an ensemble of 6 integrations of the Hadley Centre atmospheric climate model (HADAM1) for the period 1949-93. The model was forced by the Hadley Centre's observed global sea-ice and sea surface temperature data set (GISST). The model reproduces with considerable skill the patterns of many of the main modes of mean sea level pressure (MSLP) variance over this region, including the North Atlantic Oscillation (NAO).

For MSLP, the most predictable modelled seasons over the North Atlantic/European sector as a whole are spring and winter (although random variability is still substantial), and for the NAO specifically, the model shows significant skill in spring. From late winter to spring, the observed NAO is related to SST patterns mainly in the North Atlantic, and in years of extreme Atlantic SST anomalies, reasonably skilful statistical simulations of the sign of the NAO anomaly can be made. For the UK, the highest simulation skill is for temperature, which we hypothesize is directly related to local SST anomalies.

The effects of ENSO have also been investigated. Over the North Atlantic, the model produces a strong 500hPa height response to extreme El Nino events in winter and spring, similar to that observed, whereas over Europe influences are weak. The response to La Nina is very weak in both observed and simulated data.

1. Introduction

The North Atlantic/European (NAE) region is typical of the extratropics in that, on time-scales of short to medium-range forecasts, the weather is dominated by synoptic events and transitions between flow regimes (e.g. Palmer 1993, Plaut and Vautard 1994). On these time-scales, due to non-linear dynamics, unforced atmospheric variability dominates and the limit of predictability for synoptic events is probably near 10-20 days. Below this limit, short range forecasts have a strong deterministic component so they can be regarded as forecasts of the first kind (Lorenz 1975). Thus, an accurate representation of the initial atmospheric conditions is crucial. By contrast, on medium-range and monthly time-scales, predictions are more concerned with persistence of the current weather regime and the possibility of forecasting the next one or two regime transitions. These forecasts are also sensitive to the initial atmospheric state. Monthly forecasts may be regarded as predictions the second kind (Lorenz 1975) for daily weather but perhaps predictions of the first kind for regimes; the fundamentally probabilistic nature of both medium-range (Mureau et al. 1993) and monthly forecasts (Harrison 1995) is being increasingly recognised.

On the seasonal time-scales discussed in this paper, predictions of the atmosphere are essentially of the second kind. A seasonal forecast ideally predicts deviations of residence times and frequencies of prominent regional weather regimes from a suitable climatological average, though with little regard to sequence. In practice, operational seasonal forecasting to date has been mostly restricted to prediction of the seasonal mean departure from average. One well known example of a weather regime is the Pacific North American (PNA) pattern, which is known to be partially (but by no means wholly) influenced by ENSO (e.g. Horel and Wallace 1981, Ropelewski and Halpert 1986 and Livezey 1990), and can also last up to several weeks (Dole and Gordon 1983). In some parts of the USA and Canada, this pattern is sufficiently predictable in late winter to enable probabilistic seasonal temperature forecasts to be issued with reasonable skill, thus, for example, reducing costs to the gas industry (Livezey 1990). Forecasts over the NAE region of similar skill would also clearly be of great commercial benefit.

In this initial study of the NAE area, we consider only the seasonal mean response and confine our attention to *potential* predictability obtained from knowledge of concurrent SSTs and sea-ice extents. In practical predictions, SST anomalies are imperfectly known for the season ahead and so predictability is (slightly) reduced. These SST anomalies can be estimated either by persisting initial anomalies (e.g. Rowell et al. 1992), by persisting standardised anomalies to allow for the intraseasonal climatology of SST variance, by making more complex predictions of SST from a mix of statistical and dynamical techniques (e.g. Davey et al. 1994), or by using the new generation of fully coupled models (Hunt et al. 1994, Ji et al. 1994).

Predictability over the NAE sector arising from SST anomalies in both the Atlantic and Pacific Oceans has already been partially investigated. Concerning the Atlantic influence, studies of particular importance include the observational work of Ratcliffe and Murray (1970), Maryon and Storey (1985) and Deser and Blackmon (1993). Also, Kushnir (1994) and Bjerknes (1964) have noted that links differ on interannual and interdecadal time-scales; for the latter, the influence of local atmospheric circulation on SST was more pronounced than the reverse process. Van Loon and Madden (1981), Hamilton (1988) and Fraedrich and Muller (1992) have investigated the effects of ENSO on climate in the NAE sector. Some links have been found, but are much weaker than those for North America and Canada. Furthermore,

Maryon and Storey (1985), and updated work by Folland and Woodcock (1986), used SST anomalies in both the tropical Pacific and Atlantic as part of an empirical monthly forecasting system for the UK.

Modelling studies such as Palmer and Sun (1985), Brankovic et al. (1994) and Ferranti et al. (1994) have also shown the influence of SST on the NAE region, including support for an influence of SSTs near Newfoundland on winter European circulation similar to the studies quoted above. More recently, ensembles of multi-decadal integrations forced by time-varying observed SST data sets have been used to study global and regional climate variability, e.g. Dix and Hunt (1995), Harzallah and Sadourny (1995), Smith (1995), Stern and Miyakoda (1995) and Rowell (1996). The ensemble technique provides a powerful tool for analyzing variability and predictability. This paper is the first to use an ensemble of multi-decadal runs, forced with observed SST, to study seasonal variability and predictability over the NAE region.

In section 2 we document the model and experimental design, and in section 3 evaluate the model climatology, including its low-frequency modes over the NAE sector. In section 4, we study the model's predictability and simulation skill, and in section 5 relate these to patterns of SST forcing. Finally, interannual variations of predictability are investigated in section 6, and conclusions presented in section 7.

2. Experimental Design

The Hadley Centre atmospheric climate model used here is known as HADAM1, and is identical to the model first submitted to the Atmospheric Model Intercomparison Project (AMIP) (Gates 1992). It has a resolution of 2.5° latitude by 3.75° longitude, 19 hybrid levels in the vertical (5 of which represent boundary layer processes), and 4 soil levels which allow vertical heat transport within the land surface. A one layer land surface hydrology scheme parameterizes surface moisture storage, surface runoff and sub-surface runoff, and a prescribed vegetation canopy also influences surface hydrology. The convection scheme has a stability dependent closure and the cloud scheme uses prognostic variables of large-scale cloud amount, convective cloud amount, liquid water concentration and ice concentration. The radiation scheme resolves 4 long-wave bands, 6 short-wave bands, fixes atmospheric CO_2 concentration at 321 ppmv, varies stratospheric ozone with season and latitude, and responds to the four prognostic cloud variables. Further details are given by Phillips (1994).

The simulations used here are the same 6-member ensemble employed by Rowell (1996). Each member was integrated from 1st October 1948 to 1st December 1993 with lower boundary forcing supplied by the first version of the Global sea-Ice and Sea Surface Temperature data set (GISST; Parker et al. 1995). The initial atmospheric state and surface temperature were taken from UK Meteorological Office analyses for 6 different dates, arbitrarily chosen, but all close to October 1st. Soil moisture and snow depth were initialised from an adaption of the Willmott et al. (1985) climatology.

Due to likely spin-up effects, the first two months of each integration were discarded, leaving 6 x 45 = 270 years of model data, starting on December 1st 1948 and finishing on November 30th 1993.

3. Model Validation

a) Model seasonal-mean climatology

The appropriateness of a model's response to SST depends in part on the accuracy of various aspects of its climatology (e.g. Palmer and Anderson 1994). Here we assess the climatologies of model variables of interest in this paper. Fig.1 compares observed and simulated mean sea level pressure (MSLP) seasonal climatologies over the NAE region. The observed 1961-90 climatology is calculated from an early version of the new Basnett-Parker MSLP data set (Basnett and Parker 1995), while the model climatology is an ensemble mean of the 6 runs for 1961-90. In general, the model climatology compares well or very well with that observed, with spatial correlations varying from 0.97 to 0.87 (Table 1).

Some biases and errors can be seen. The position of the Azores high is well modelled in spring, summer and autumn, but in winter is displaced to the east into northwest Africa. In summer the centre of the Azores high is too intense. The modelled Icelandic low is displaced about 3° latitude to the southwest of that observed in winter, and about 5° south in spring, giving errors of up to 4hPa in the North Atlantic. In all seasons, except summer, the depression track extending towards the Barents Sea is too weak. This gives MSLP values that are too high over Scandinavia, especially in spring, with slack gradients resulting in insufficient winds from the southwest. In all seasons, modelled pressure over Greenland appears to be several hPa too low, although this may be partly due to differences in the reduction of surface pressure to mean sea level.

Fig.2 shows the observed and modelled 500hPa 1961-90 climatologies. The observed data is taken from UK Met. Office analyses. Table 1 shows that 500hPa height is simulated about as well as MSLP. The model has errors of less than 60m in most places and mean flow strength is generally close to that observed, except near Greenland where it is too weak in all seasons except summer. One fairly consistent pattern of model bias, which occurs throughout the year, is of anomalously low heights from approximately 40°-50°N and anomalously large heights further north. This is especially true in winter and spring where the error reaches a maximum of 80m at 45°N, 30°W, and occurs because the model extends the Canadian trough too far east and gives excessive Arctic 500hPa heights.

The modelled screen level air temperature climatology for 1961-90 (not shown) has been compared with a merged 1961-90 climatology over land (Jones 1994) and an updated version of the night marine air temperature climatology of Bottomley et al. (1990) (D.P. Cullum, personal communication, 1995). Modelled seasonal surface air temperature is, not surprisingly, very well simulated with spatial correlations between 0.91 and 0.96. Some biases are however seen over land. The model is 1-4°C too cold over Scandinavia in all seasons, and several degrees too cold over central and western Europe in winter. In summer, central and eastern Europe are 2-4°C too warm, giving too large a seasonal temperature range. This is consistent with a lack of westerlies from the Atlantic penetrating this region, which would moderate summer and winter temperature extremes.

Modelled precipitation for the same period has been compared with the 'timeless' Legates and Willmott (1990) precipitation climatology which is bias-adjusted over land. Precipitation is a difficult field to model (e.g. Rowell 1996), but Table 1 shows that the spatial correlations consistently exceed 0.70. Again, some clear biases are seen; the model is 1-3mm/day too dry from autumn to winter over the UK and north Atlantic, 1-2mm/day too dry in summer over central and eastern Europe, and 1-2mm/day too

wet in all seasons over Scandinavia. However the poor resolution of mountains in the model and the uncertainty of observations over ocean areas prevent further meaningful comparisons.

Overall, it is concluded that the model's mean climatology has no serious errors over the NAE region.

b) Model variability over the North Atlantic/European region

The variability of seasonal MSLP has been analysed by separately applying an unrotated covariance eigenvector (EOF) analysis to the observed and modelled data sets for each of twelve overlapping 3-month seasons. EOFs were calculated using an equal-area grid of approximately 500km latitude by 700km longitude over the area 20°N-80°N, 75°W-40°E, using temporally unfiltered data. Rotation of the EOFs was rejected because the first unrotated EOF for every season was a readily recognisable dipole pattern (see below) which rotation tended to confound with other patterns. This is not surprising over the limited domain used here, as rotation tends to over-regionalise patterns which are in reality domain-wide.

Figs.3a-d show observed EOF1 for the four standard seasons (December-February, March-May etc.) using 1949-93 data, while figs.3e-h show modelled EOF1 calculated from all 270 years of model data. The naming convention is such that 'OBS-DJF1' denotes the first EOF of observed winter MSLP, 'MOD-MAM3' is the third EOF of modelled spring MSLP, etc. The percentage of variance explained by each pattern is shown at the top of each diagram and in Table 2.

Fig.3a (OBS-DJF1) is a north-south dipole pattern which well represents the North Atlantic Oscillation (NAO) in winter (e.g. Wallace and Gutzler, 1981, Barnston and Livezey 1987, Hurrell 1995) and accounts for almost half (49%) the total variance. The first EOFs in the other seasons (figs. 3b-d) are also dipole patterns, although with additional fine-scale detail, and represent a smaller fraction of total variance (lowest in SON at 30%). In summer, the positive centre of the NAO shifts north to around 45°N over the Atlantic and 50-55°N over Europe with an extra band of weak negative values over North Africa. A similar seasonal cycle of the NAO centres of action was documented by Barnston and Livezey (1987) in a rotated EOF analysis of observed hemispheric 700hPa height data. Figs.3e-h show corresponding model patterns of EOF1; these match the seasonally varying observed patterns very well as indicated by the spatial correlations in Table 2.

Lower order EOFs also represent a significant fraction of variance; fig.4 show EOFs2-4 in winter. Figs.4a,d show OBS-DJF2 and MOD-DJF2, representing 16% and 18% of the variance respectively. These match the East Atlantic pattern of Barnston and Livezey (1987), and Table 2 shows they are highly correlated (r=0.92). Figs.4b,e show OBS-DJF3 and its model counterpart, MOD-DJF4, which are also well correlated (r=0.87). This pattern appears in a fairly similar form in all other standard seasons as EOF3 in both model and observations, and its positive phase can be identified with Scandinavian blocking. Figs.4c,f show OBS-DJF4 and its counterpart, MOD-DJF3, correlated at r=0.66. Both EOFs explain 9% of their respective variances and show a wavetrain-like response emanating from an area near Newfoundland with negative weights over western Europe, and positive weights over much of Scandinavia and western Russia; this is similar to the response identified by Ratcliffe and Murray (1970) and Palmer and Sun (1985) to SST variations near Newfoundland. Broadly similar patterns are seen in the other standard seasons in both model and observations, although are sometimes partly phase shifted. Overall, these results and Table 2 show the model reproduces the main modes and their seasonal cycle of variability

in the NAE region well in winter and autumn, and somewhat less well in spring and summer except for spring EOF1 (the NAO) which is very well captured.

To further analyse the variability of surface westerly flow over the North Atlantic, an index was formed by subtracting the observed MSLP nominally at Stykkisholmur, Iceland (65.1°N, 22.7°W) from that at Ponta Delgada, Azores (37.8°N, 25.7°W) (cf. Hurrell and Van Loon 1993). Model and observed values were interpolated from the gridded data (observed values are particularly accurate near these points). Note that this 'westerly index' has an interannual temporal correlation of 0.96 with the winter EOF1 in January, but not surprisingly correlations with the summer EOF1 time series fall to 0.60 in July. Fig.5 shows the monthly mean values of the westerly index and their interannual standard deviations over 1949-93. Both observed and model indices have a minimum in May (when the Greenland high is strongest), but the model maximum occurs in September, rather than December as observed, because the model Iceland low is displaced too far south near Iceland (fig.1). Interannual variability of the index is generally well simulated through the seasonal cycle, with a minimum of variability in July/August as observed, though the modelled maximum variability (February/March) is a little later and rather weaker than observed (January).

4. Model Predictability

a) Impact of SSTs on the North Atlantic/European region

We use analysis of variance (ANOVA), following Rowell et al. (1995) and Rowell (1996), to provide quantitative estimates of seasonal predictability. A general discussion of ANOVA can be found in many texts e.g. Scheffe (1959) or Afifi and Azen (1979). Here we use ANOVA to estimate the percentage of total seasonal variance caused by SST/sea-ice forcing, ie. that variance common to all runs (note that autocorrelation of the forcing has only a minor effect on estimates of this percentage). The remaining variance is attributed to unforced internal atmospheric variability or atmospheric 'chaos'. We make no attempt to distinguish between atmospheric chaos and the influence on the atmosphere of simulated soil moisture interactions; this would require an experimental design with additional integrations having prescribed land surface forcing. A fraction of the internal atmospheric variability may be affected in this way, and so could potentially exhibit a little extra predictability (probably mainly in summer). Significance testing is performed by testing the null hypothesis that the variance caused by oceanic forcing is not significantly greater than zero (Rowell, 1996). A statistically significant rejection of this null hypothesis can be thought of as the first stage towards revealing the potential for this model to be used in practical seasonal prediction. A further condition is the size of its interannual simulation skill verified against observations; see section 4b.

Fig.6 shows the estimated fraction of total variance attributed to SST/sea-ice forcing for seasonal MSLP by applying ANOVA to the 6 model runs for 1949-93. The 95% significance level for non-zero ocean forcing is about 7%, and areas exceeding this are shaded. Low but significant values are found over large parts of the NAE region in all seasons; north of 40°N values are generally in the range 0-20%, whereas over the sub-tropical Atlantic they reach 50-60%. MSLP predictability measured in this way is generally highest in spring (MAM), where centres exceeding 20% are seen near Iceland and over southeast Europe, and also reach 60% over parts of the sub-tropical Atlantic. The larger spring predictability over

Europe agrees with Brankovic et al. (1994) and Palmer and Anderson (1994), who explain this as being due to lower internal variability in spring compared to winter but also potential vorticity gradients (important for teleconnections from the tropics) which are almost as strong in spring as in winter. Another centre of higher predictability (about 18%) is seen in winter (DJF) just southwest of Ireland. The remaining seasons (JJA and SON) have generally lower MSLP predictability.

Fig.7 shows ANOVA values for model 1.5m air temperature in the four standard seasons. Values over Europe are generally 5-15%, but often greater (near 20%) over parts of the UK, Scandinavia and around the Mediterranean. Over the oceans, values are not surprisingly much higher, rising to over 90% southwest of the UK in summer and over the sub-tropical Atlantic in all seasons, although values are considerably lower in winter north of 30°N. Over land, the extra predictability near European coasts is probably due to the *direct effect of adjacent SST anomalies*. This is regularly used via empirical equations in real-time monthly temperature predictions for the UK (Folland et al. 1986 and T.P. Legg, personal communication, 1993), which, like fig.7, show the weakest direct influence of coastal SSTs on the UK is in winter.

ANOVA calculations for precipitation (not shown) generally yield lower variance values (0-12%) over European land areas, but with a tendency for higher predictability in southern rather than northern Europe. Model 500hPa height ANOVA maps (not shown) are broadly similar to those for MSLP (fig.6), except that values are generally several percent lower and areas of significant ocean influence are slightly smaller. This indicates that, at least for this model, there may be no advantage in using 500hPa height rather than MSLP for European seasonal prediction.

Section 3b showed that the first EOF of MSLP variability in the NAE region consistently represents the NAO through the whole year, although with variations in pattern from winter to summer. We have investigated the predictability of the NAO mode on both monthly and seasonal (3-month mean) time-scales. EOF1 was separately computed for all 12 calendar months and 12 overlapping seasons and ANOVA applied to the EOF1 time coefficients. The resulting annual cycle of percentage variance explained by SST and sea-ice forcing is shown in fig.8. Seasonal values of variance explained are, not surprisingly, generally higher than monthly ones (see discussion in Rowell 1996) peaking at 16% in spring (MAM), with the lowest values in summer (JJA). There is also a secondary peak in early autumn (ASO) and a secondary seasonal minimum in late autumn (OND). For the westerly index, ANOVA yields the same maxima in spring and autumn with a minimum in summer, but the values of variance explained are more variable from season-to-season and usually less than those of the EOF-based index. These differences may be real or due to random sampling effects.

b) Model interannual skill of the North Atlantic/European region

ANOVA shows when and where the model ensemble responds with at least some consistency to SST forcing. However for practical model-based prediction, a necessary further step is to evaluate whether or not the consistency of model responses to ocean surface forcing can translate into skill at simulating observed variations in climate. For MSLP, we measure this skill, at each grid point, by correlating model ensemble mean MSLP anomalies with corresponding observed anomalies from the Basnett-Parker MSLP data set for the period 1949-93. However, the skill at each point is limited by (and related to) internal atmospheric variability even if the model is responding perfectly to SSTs. This relationship needs to be

defined for a meaningful assessment of the model's skill, and for a perfect model, Rowell (1996) shows that the (standard) correlation between ensemble means and observed data, r_{EM}, is related to the fraction of forced variance (ρ) as follows:

$$r_{EM} = \rho n^{1/2}(\rho(n - 1) + 1)^{-1/2} \quad (1)$$

where n is the ensemble size. For n=6, this gives $r_{EM} \sim 2\rho$ for $\rho \leq 0.2$. In general, the correlation skill of an imperfect model would be less than this theoretical value, although it is also conceivable that a model with more internal variability than the real atmosphere (ie. ρ too low) might exceed this value (since r_{EM} from equation 1 would also be too low).

Fig.9 shows the standard correlations between observed and simulated MSLP anomalies over 1949-93 for the four standard seasons. Areas statistically significant, allowing for autocorrelation, are shaded. In DJF, correlations vary between -0.2 and 0.5 over land (highest values are over western Europe and north Africa), increasing to 0.7 over the tropical Atlantic. Correlations of up to 0.45 appear over the Bay of Biscay, the UK and western Europe and these areas fit fairly well with ANOVA patterns in fig.6a. There is no significant correlation skill (at grid point resolution) over the remainder of mainland Europe. MAM shows two large areas of significant skill centred over south Greenland and the sub-tropical Atlantic whose location and magnitude match the ANOVA patterns in fig.6b. There is no correlation skill over Europe in JJA or SON. In general, skill is a little less over Europe than might be expected from the ANOVA results, suggesting that some of the model's teleconnections from SST forcing may not be correct.

Fig.10 shows standard correlations between modelled 1.5m air temperature and observed air temperature. These are fairly consistent with the ANOVA maps of fig.7, and model skill by this measure often exceeds 0.3 over land. Following our comments above (section 4a), the higher skill around coastal Europe presumably results from the advection of temperature anomalies from nearby seas. Some systematic differences from the ANOVA-expected results are however apparent: in winter, correlations are higher than anticipated over much of western Europe (Scandinavia, U.K., western France and Iberia) and also over North Africa, whereas for inland Europe, in all seasons except autumn, correlations are generally less than expected. The poor summer skill may be due to erroneous drying of the model land surface in this season. Other smaller and less coherent differences from ANOVA-expected results are probably due to sampling error.

Time series of the model's ensemble mean NAO have also been correlated with observed NAO time series, using the MSLP EOFs described in section 3b for all 12 overlapping 3-month seasons (note that the model and observed NAO EOF patterns are sufficiently similar to make this comparison valid). Fig.11 shows that the highest correlations are in winter and spring, reaching 0.31 for FMA and MAM. This is significant at the 95% level (allowing for autocorrelation), and is consistent with the maximum skill expected from the variance due to SSTs (fig.8 and equation 1). Interestingly, the model shows no significant correlation skill in ASO where a secondary ANOVA peak was found, indicating that there may be some errors in model teleconnections to SST. When the westerly index is used, a similar annual cycle of skill is found, with correlations again peaking in spring.

5. Ocean - Atmosphere Links

We now investigate in more detail some of the links between SST anomaly patterns and atmospheric circulation over the NAE region, concentrating on features shown to have predictability in

section 4.

Up to this point, we have utilised data which are unfiltered in time; this is often appropriate, since what the atmosphere 'sees' are spatial patterns of unfiltered SSTs with little knowledge of their temporal context beyond a few months. However, different coupling mechanisms and ocean-atmosphere relationships may exist on different time-scales, and it can be argued that for the purpose of investigating specific SST patterns linked to seasonal predictability, data should first be filtered to exclude interdecadal signals (c.f. Barnston 1994). Fluctuations in forcings on different time-scales can give rise to different seasonal to decadal predictabilities. This may be particularly true of the North Atlantic, where for example, thermohaline variations can substantially influence SST and atmospheric circulation on decadal time-scales (e.g. Dickson et al. 1988, Mysak et al. 1990, Wohlleben and Weaver 1995).

Here, we exclude time-scales close to or greater than the decadal, so including the usual time-scales associated with ENSO. We apply a high-pass 10-point non-recursive filter (Walraven 1984), with 50% amplitude point at 8 years, to all atmospheric and SST data described below.

Two approaches are taken to investigate the large-scale links between SST variations and seasonal atmospheric anomalies. In the first, a prominent feature of atmospheric variability is chosen - here it is the NAO (see section 5a) - which is then related to grid point SST variations. In the second and converse approach, a prominent aspect of SST variability is selected - here it is ENSO (see section 5b) - which is then related to grid point atmospheric variations over the NAE region. This second approach could also be used for the much smaller Ratcliffe-Murray (1970) area near Newfoundland, but the more complex influence of this region on climate is considered beyond the scope of this paper.

a) Links between the NAO and Atlantic SSTs

Relationships between the NAO and Atlantic SSTs are investigated here using a compositing technique. Covariance EOFs were calculated from the observed and modelled high-frequency (HF) seasonal MSLP data on the same grid as used in section 3b, and the EOF1 patterns were again found to represent the NAO, being almost identical to those in fig.3. For each season, the 10 most positive (high NAO) and 10 most negative (low NAO) EOF1 time coefficients for 1949-93 were chosen from the observed EOF1 time series and from the model ensemble mean time series. For each of these sets of years (model or observed, high or low NAO) an SST composite was formed using HF SST anomaly data. The null hypothesis, that the mean SST anomaly pattern is the same for high and low NAO years, was tested for model and observed composites at each grid point using a 2-tailed t-test, taking account of autocorrelation in the SST data (even though much of this autocorrelation is removed by the filtering).

Figs.12a,b show differences between the mean SST in high and low NAO years, using observed and modelled NAO data respectively for MAM. This is the season of highest model NAO predictability (measured by ANOVA and temporal correlation skill; section 4). The model and observed composite patterns are very similar (their spatial correlation is 0.75), and where the model shows local statistical significance this implies support for a real atmospheric response to the pattern of anomalies shown. Note however, that some of the observed pattern may also arise from a positive feedback whereby the atmosphere also cools or warms the ocean. A lag correlation analysis (not shown) was unable to resolve this issue, but it may be argued that the horizontally banded structure of SST differences lends support to this view. For example, when the NAO is positive, enhanced northwesterly winds would tend to cool

the ocean surface in the northwest Atlantic (40°-50°N), enhanced subsidence to the south may reduce cloud cover and so warm the subtropical Atlantic, and stronger northeasterly trades could perhaps cool north tropical SSTs as observed. Coupled model experiments are clearly needed to disentangle these effects. This pattern of SST anomalies is also a well-known mode of Atlantic variance (e.g. Lau and Nath 1990, Deser and Blackmon 1993, Kushnir 1994), and its tropical part has been used successfully by Ward and Folland (1991) as a main predictor for MAM Nordeste (northeast Brazil) rainfall.

In other seasons, model composite differences compare rather less well with those observed, with the exception of NDJ, where both the model and observed composites have similar but weaker banded structures to those of MAM. This may however be a chance result in NDJ, since SSTs seem to have a negligible impact on the NAO at this time of year (fig.8). In the remaining seasons, the lack of similarity between model and observed composites probably simply reflects the highly chaotic nature of interannual variations of the NAO (fig.8), although in early-autumn it may also reflect model error (c.f. section 4b).

b) Links between ENSO and North Atlantic/European seasonal variability

The possible effects of ENSO on NAE climate have been documented by several authors (e.g. Van Loon and Madden 1981, Hamilton 1988 and Fraedrich and Muller 1992). They all used the Southern Oscillation Index (SOI) to measure ENSO, and generally found only weak composite responses over Europe and the North Atlantic. Here, we measure ENSO with a Pacific SST index defined by the first unrotated covariance EOF of Pacific SSTs over 50°N-50°S, 150°E-75°W, similar to the index used by Ward and Folland (1991) for Nordeste (northeast Brazil) rainfall studies. This has the advantage of explicitly representing the pattern of ENSO-related SST forcing, rather than using an atmospheric proxy such as the SOI. Separate EOF patterns were created for each of the 12 overlapping seasons from HF SST data for 1949-93, and using these time series, the 10 highest (most La Nina-like) and 10 lowest (most El Nino-like) years were identified for each season. From these sets of years, composites of HF 500hPa heights were calculated for each overlapping season over the NAE region for observed data (UK Met. Office analyses) and model ensemble mean data. Statistical significance of the composite anomalies (El Nino years minus all years, La Nina years minus all years, and El Nino years minus La Nina years) were computed using a 2-tailed t-test. (Note that the whole analysis was also repeated with the 5 strongest El Nino and La Nina years, but significance was generally reduced.)

First we discuss the observed El Nino composites. The most significant impacts north of 30°N over the NAE are found in JFM, FMA and OND. JFM has the strongest response over the North Atlantic (fig.13a), with greater cyclonic activity (lower 500hPa height) extending from southeastern USA towards the Azores, higher than normal heights further north, increased heights over North Africa and the Middle East, and slightly negative (but insignificant) anomalies over much of Europe, which induce anomalous north-northeasterly flow over the UK. (Note that FMA shows a broadly similar response pattern, and to some extent MAM). Westerly flow over the west and central North Atlantic is thus weakened (reminiscent of the 'TNH' mode of Livezey and Chen 1983), and although this is similar to the ENSO signal of Hamilton (1988), Van loon and Madden (1981) and Palmer and Anderson (1994), the dipole found here does not extend as far into the northeast Atlantic.

During OND, the observed response to El Nino (not shown) is dominated by a significant drop of heights from northwest Canada and Greenland to the UK (leading to anomalous 500hPa southerly flow

over the UK), with weaker but significant falls further south over the subtropical North Atlantic. In NDJ, a weakly significant increase of heights (not shown) is found over and to the west of the UK, which would induce southerly anomalies over the UK. Interestingly, these results may possibly reflect a long-held opinion among former UK long-range forecasters that a mild southerly mid-autumn tends to presage a blocked cold winter (c.f. JFM El Nino results, above).

The model's El Nino composites for DJF to FMA are encouragingly similar to those observed (figs.13a,d are spatially correlated at 0.90) and are also highly significant, thus adding weight to the NAE ENSO impact described above. The model response in OND is weaker than observed, and the response in NDJ is quite different to that observed.

Observed La Nina responses are generally much weaker (and less significant), although the JFM and FMA patterns are opposite to those for El Nino over the western Atlantic (fig.13c for JFM). The model responses are generally broadly similar to those observed, but are usually more significant (e.g. fig.13d). From DJF to MAM the model simulates higher than normal heights from the southeast USA to western Europe (south of about 55°N), with lower heights to the north, particularly over southern Canada and Greenland.

The El Nino - La Nina difference patterns are not surprisingly more like those for El Nino given its stronger response (e.g. fig.13e,f). The response to ENSO therefore seems somewhat non-linear. This may be because the character of SST anomalies is not exactly reversed between La Nina and El Nino events, with La Nina usually having a narrower pattern of equatorial anomalies. However, the possibility that this difference may also create problems with our analysis should be noted. First, the Pacific SST EOF pattern used here is probably biased more towards El Nino events, and second the SST data set used to define the composite years, GISST1, has been found to insufficiently represent the scale and sharpness of some La Nina anomalies during 1949-93, compared to the new GISST2 data set (N.A. Rayner, personal communication, 1996). Furthermore, the model response to these SSTs may be adversely affected via tropical Pacific diabatic heating anomalies; this clearly demands investigation.

We conclude that ENSO affects the NAE region in at least the winter half-year. A more detailed investigation is needed, including an analysis of model simulations forced with the new GISST2 data set.

6. Temporal variations in predictability of NAO

Section 4 showed that overall, the NAO as defined by the time coefficient of MSLP EOF1 had some predictability in winter and spring. This was related to SST patterns in the North Atlantic (section 5), though we also suspect some influence from ENSO on at least part of the NAO pattern. We now investigate (for winter and spring) whether NAO predictability is larger in years with stronger Atlantic SST patterns (see Rowell 1996 for a definition and further discussion of interannual variations of predictability).

For each of 5 overlapping seasons, the 45-year period was split into five categories of 9 years each, according to the amplitude of the first unrotated covariance EOF of Atlantic (30°S-80°N, 80°W-30°E) HF SSTs for 1949-93 (computed separately for each season). Category 1 years have strong SST anomaly patterns broadly resembling fig.12, whilst category 5 years have strong anomalies which are roughly the reverse of this. Table 3 shows the number of years in each category of SST forcing for the seasons DJF to AMJ for which an above/below average observed HF NAO time coefficient was seen in that season. An

appropriate null hypothesis to test is that there are equal numbers of above or below average NAO years regardless of category. A χ^2 value and its significance level was calculated for each season (table 3), and the method of Craddock and Flood (1970) used to allow for the small numbers in each category (less than 5 if need be). Since the prior expectation is that near-average categories have little or no discriminating power, then the inclusion of category 3 results should lead to conservative results.

Table 3 shows that χ^2 is most significant in JFM and FMA. For JFM to AMJ, category 1 SSTs (ie. similar to fig.12a) are associated with a strong tendency towards positive NAO anomalies. Category 5 SSTs have a similarly strong reverse effect in JFM and FMA, but a much weaker effect in MAM and AMJ. Thus in years of extreme late winter (and to some extent spring) Atlantic SST anomalies (defined by the phase of Atlantic SST EOF1), the sign of the observed NAO seems to respond more consistently to ocean forcing. This has important implications for seasonal prediction in such years.

Table 4 shows an identical analysis using the simulated ensemble mean NAO. These results are much weaker than observed, with only FMA significant at the 95% level, although the model is qualitatively correct for categories 1 and 5 from JFM to AMJ. Possible reasons for this are that the model response may be too weak, or that the observed discrimination is too strong for predictive purposes because it may include a substantial influence of the atmosphere on the ocean. Nevertheless, the model results again indicate that the Atlantic ocean does have a role in forcing the NAO.

7. Summary and discussion

We have studied an ensemble of 6 runs of the Hadley Centre AGCM (HADAM1) integrated from 1949-93 forced by historic SSTs and sea ice from the GISST1 data set. Each run was started from a different set of initial atmospheric conditions. We have concentrated on quantifying seasonal predictability in the North Atlantic and European (NAE) region with the aim of finding the times of the year and locations where there is useful predictability and skill.

The model has good MSLP and 500hPa height climatologies over the NAE region, with a similar seasonal cycle to that observed. The model also correctly reproduces the area's leading mode of interannual variability, the NAO, with a good simulation of the seasonal cycle of its pattern and interannual variance. Several other modes, some of which have been recognised in other studies, are also reproduced well by the model.

The model shows the most predictable seasons for MSLP and 500hPa height over the NAE to be spring and winter. For these variables, there are weak but significant skill maxima in winter (DJF) over western Europe and over the North Atlantic in spring (MAM). Time series of the NAO also showed maximum predictability and skill in MAM. Over coastal Europe, temperature seems to have useful predictability (except perhaps in summer), probably due to the direct influence of nearby SST anomalies.

Interannual variance of the observed and modelled NAO in spring was found to be primarily linked with a fairly well known pattern of tropical/North Atlantic SST anomalies which exhibits a dipole structure across the equator and a quasi-zonal banded structure to the north. In particular, it was shown that if this mode of Atlantic SST variability is in an extreme phase, then it is possible to simulate with moderate accuracy the sign of the late winter to spring NAO anomaly.

The effects on the NAE region of SST anomalies in the tropical Pacific are dependent on both the sign of anomalies and the season. In late winter and much of spring, El Nino affects the pressure pattern

over the northwestern Atlantic, tending fill the western part of the Icelandic low and weaken the Bermuda high. The model reproduces this well. The influence of La Nina events on the NAE may be rather weaker. Over the UK, we tentatively conclude that 500hPa flow may be affected by ENSO for as much as half the year, from autumn to spring.

Overall, we feel the analysis presented here indicates that further work on seasonal predictability over Europe is justified, particularly over coastal Europe and including the UK. This should take advantage of current developments in models and SST data sets. One potentially significant set of factors that may be important for future seasonal prediction are anthropogenic pollutants of the atmosphere, such as increasing carbon dioxide, tropospheric aerosols, and changes in stratospheric and tropospheric ozone. Furthermore, the partial ambiguity of relationships between SSTs and the NAO uncovered here indicate that a three-pronged approach using observational data, atmospheric models forced with ocean surface data and other factors, and coupled models, is the best way forward.

Acknowledgements. We thank R.E. Livezey for valuable discussions about the annual cycle of extratropical northern hemisphere seasonal predictability. Gridded observed MSLP data was kindly provided by T. Basnett and D.E. Parker, and D.P. Cullum provided the air temperature data. A.C. Renshaw and D. Sexton provided helpful comments, ran the model integrations and wrote some of the software. Computer time was provided by the UK Department of Environment, under contract PECD7/12/37, with further partial support under CEC contract EV5V-CT92-0121 ("Medium Term Climate Variability").

REFERENCES

Afifi, A.A. and Azen, S.P., 1979: Statistical Analysis - a computer orientated approach. Second Edition. Academic Press. 442pp.

Barnston, A.G. 1994: Linear statistical short-term climate predictive skill in the Northern Hemisphere. J. Climate, 7, 1513-1564.

Barnston, A.G. and Livezey, R.E., 1987: Classification, seasonality and persistence of low-frequency atmospheric circulation. Mon. Wea. Rev., 10, 1083-1126.

Basnett, T.A. and Parker, D.E., 1995: A provisional new global mean sea level pressure data set. In: Folland, C.K. and Rowell, D.P. (eds), 1995: Workshop on simulations of the climate of the twentieth century using GISST, 28-30 November 1994, Hadley Centre, Clim. Res. Tech. Note No. 56, 58-60.

Bjerknes, J., 1964: Atlantic air-sea interaction. Adv. Geophys., 10, 1-82.

Bottomley, M., Folland, C.K., Hsiung, J., Newell, R.E. and Parker, D.E. 1990: Global Ocean Surface Temperature Atlas "GOSTA". Publication funded by UK Depts of Environment and Energy for the Intergovernmental Panel on Climate Change. HMSO, London, 20pp+iv, 313 plates.

Brankovic, C., Palmer, T.N. and Ferranti, L., 1994: Predictability of seasonal atmospheric variations. J. Climate, 7, 217-237.

Craddock, J.M. and Flood, C.R., 1970. The distribution of the χ^2 statistic in small contingency tables. Journal of the Royal Statistical Society Series C (Applied Statistics), 2, 173-181.

Davey, M.K., Ineson, S. and Balmaseda, M.A., 1994: Simulation and hindcasts of tropical Pacific Ocean interannual variability. Tellus, 46A, 433-447.

Deser, C. and Blackmon, M., 1993: Surface climate variations over the North Atlantic Ocean during winter 1900-1989. J. Climate, 6, 1172-1180.

Dickson, R.R., Meincke, J., Malmberg, S-A, and Lee A.J., 1988: The "great salinity anomaly" in the northern North Atlantic 1968-1982. Prog. Oceanogr., 20, 103-151.

Dix, M.R. and Hunt, B.G, 1995: Chaotic influences and the problem of deterministic seasonal predictions. Int. J. Climatol., 7, 729-752.

Dole, R.M., and N.D Gordon 1983: Persistent anomalies of the extratropical Northern Hemisphere wintertime circulation: Geographical distribution and regional persistence characteristics. Mon. Wea. Rev., 111, 1567-1586.

Ferranti, L., Molteni, F. and Palmer, T.N., 1994: Impacts of localised tropical SST anomalies in ensembles of seasonal GCM integrations. Q. J. R. Meteorol. Soc., 120, 1613-1647.

Folland, C.K. and Woodcock. A. 1986: Experimental monthly long-range forecasts for the United Kingdom: Part I, The forecasting system. Met. Mag., 115, 301-318.

Fraedrich, K. and Muller, K., 1992: Climate anomalies in Europe associated with ENSO extremes, Int. J. Climatol. 12, 25-31.

Gates, W.L., 1992: AMIP: The atmospheric model intercomparison project. Bull. Am. Met. Soc., 73, 1962-1970.

Hamilton, K., 1988: A detailed examination of the extratropical response to tropical El Nino/Southern Oscillation Events. J. Climatol., 8, 67-86.

Harrison, M.S.J., 1995: Long-range forecasting since 1980: Empirical and numerical prediction out to one month for the United Kingdom. Weather, 50, 440-449.

Harzallah, A. and Sadourny, R., 1995: Internal versus SST-forced atmospheric variability as simulated by an atmospheric general circulation model. J. Climate, 8, 474-495.

Horel, J.D. and Wallace, J.M., 1981: Planetary scale phenomena associated with the Southern Oscillation, Mon. Wea. Rev., 109, 813-829.

Hunt, B.G., Zebiak, S.E. and Cane, M.A., 1994: Experimental predictions of climate variability for lead times of twelve months. Int. J. Climatol., 14, 507-526.

Hurrell, J.W., 1995: Decadal trends in the North Atlantic Oscillation and relationships to regional temperature and precipitation. Science, 269, 676-679.

Hurrell, J.W. and Van Loon, H., 1993: Analysis of low frequency climate variations over the northern hemisphere using historical atmospheric data. Fourth Symposium on Global Change Studies (17-22 January 1993, Anaheim, California), Amer. Meteorol. Soc., 355-360.

Ji, M., Kumar, A., Leetmaa, A., 1994: A multiseason climate forecast system at the National Meteorological Centre. Bull. Am. Met. Soc., 75, 569-577.

Jones, P.D., 1994: Hemispheric surface air temperature variations: a reanalysis and an update to 1995. J. Climate, 7, 1794-1802.

Kushnir, Y., 1994: Interdecadal variations in North Atlantic sea surface temperature and associated atmospheric conditions. J. Climate, 7, 142-157.

Lau,N.-C, and Nath, M.J., 1990: A general circulation model study of the atmospheric response to extratropical SST anomalies observed in 1950-79. J. Climate, 3, 665-989.

Legates, D.R. and Willmott, C.J., 1990: Mean seasonal and spatial variability in gauge corrected global precipitation. Int. J. Climatol, 10, 111-127.

Livezey, R.E., 1990: Variability of skill of long-range forecasts and implications for their use and value. Bull. Am. Met. Soc., 71, 300-309.

Livezey, R.E. and Chen,W.-Y., 1983: Statistical field significance and its determination by Monte Carlo techniques. Mon. Wea. Rev., 111, 46-59.

Lorenz, E.N., 1975: Climate predictability: The physical basis of climate modelling. WMO/GARP Publ. Series No.16, 132-136.

Maryon, R.H. and Storey, A.M., 1985: A multivariate statistical model for forecasting anomalies of half monthly mean surface pressure. J. Climatol., 5, 561-578.

Mysak, L A, Manak, D.K and Marsden, R.F., 1990: Sea-ice anomalies observed in the Greenland and Labrador seas during 1901-1984 and their relation to an interdecadal Arctic climate cycle. Clim. Dyn., 5, 111-133.

Mureau, R., Molteni, F. and Palmer, T.N., 1993: Forecasts from dynamically conditioned perturbations. Q. J. R. Meteorol. Soc., 119, 299-323.

Palmer, T.N., 1993: Extended-range atmospheric prediction and the Lorenz model. Bull. Am. Met. Soc., 74, 49-65.

Palmer, T.N. and Anderson, D.T.L., 1994: The prospects for seasonal forecasting -a review paper. Q. J. R. Meteorol. Soc., 120, 755-793.

Palmer, T.N. and Sun, Z., 1985: A modelling and observational study of the relationship between seas surface temperature in the north-west Atlantic and the general circulation. Q. J. R. Meteorol. Soc., 111, 947-975.

Parker, D.E., Folland, C.K., Bevan, A., Ward, M.N., Jackson, M. and Maskell, K., 1995: Marine surface data for analysis of climatic fluctuations on interannual to century time-scales. In: Natural Climate Variability edited by D.G.Martinson et al, National Academy Press, Washington D.C, in press.

Plaut, G. and Vautard, R. 1994: Spells of low-frequency oscillations and weather regimes in the Northern Hemisphere. J. Atmos. Sci., 51, 210-236.

Phillips, T.J., 1994: A summary documentation of the AMIP models. PCMDI Report No.18, Univ. of California, Lawrence Livermore National Laboratory, Calif.

Ratcliffe, R.A.S., and Murray, R., 1970: New lag associations between North Atlantic sea temperatures and European pressure applied to long range weather forecasting. Q. J. R. Meteorol. Soc., 96, 226-246.

Rowell, D.P., 1996: Using an ensemble of multi-decadal GCM simulations to assess potential seasonal predictability. J.Climate, submitted.

Rowell, D.P., Folland, C.K., Maskell, K, Ward, M.N., 1995: Variability of summer rainfall over tropical north Africa (1906-92): Observations and modelling. Q. J. R. Meteorol. Soc., 121, 669-704.

Rowell, D.P., Folland, C.K., Maskell, K, Owen, J.A., Ward, M.N., 1992: Modelling the influence of global sea surface temperature on the variability and predictability of seasonal Sahel rainfall. Geophys. Res. Lett., 19, 905-908.

Scheffe, H., 1959: The analysis of variance. John Wiley and Sons, New York, 477pp.

Smith, I.N., 1995: A GCM simulation of global climate interannual variability: 1950-1988. J. Climate, 8, 709-718.

Stern, W. and Miyakoda, K., 1995: The feasibility of seasonal forecasts inferred from multiple GCM simulations. J. Climate, 8, 1071-1085.

Van Loon, H. and Madden, R.A., 1981: The Southern Oscillation. Part I: Global teleconnections with pressure and temperature in northern winter. Mon. Wea. Rev., 109, 1150-1162.

Wallace, J.M. and Gutzler, D.S., 1981: Teleconnections in the geopotential height field during the Northern Hemisphere winter. Mon. Wea. Rev., 109, 784-812.

Walraven, R., 1984: Digital filters. In: Proceedings of the digital equipment users society, Anaheim, California, December 1984 (unpublished document available from the Department of Applied Science, University of California, Davis, California), 23-30.

Ward, M.N. and Folland, C.K., 1991:Prediction of seasonal rainfall in the north nordeste of brazil using eigenvectors of sea surface temperatures. Int. J. Climatol, 11, 711-743.

Willmott, C.J., Rowe, C.M. and Minz, Y., 1985: A global archive of land cover and soils data for use in general circulation models, J. Climatol., 5, 119-143.

Wohlleben, T.M.H., and Weaver, A.J., 1995: Interdecadal climate variability in the subpolar North Atlantic. Clim. Dyn., 11, 459-467.

Table 1 Spatial correlation between 1961-90 model and observed climatologies over the region 30°N-85°N, 75°W-50°E. The 500hPa height climatologies were in the form of anomalies from their respective zonal means.

	DJF	MAM	JJA	SON
MSLP	0.92	0.87	0.97	0.94
Precipitation	0.71	0.71	0.73	0.73
1.5m Temperature	0.94	0.96	0.91	0.95
500hPa Height	0.92	0.89	0.86	0.97

Table 2 Spatial correlations between leading observed and modelled seasonal EOFs calculated over the period 1949-93. The variance explained by each mode is in brackets.

(a) Winter (DJF).

	Obs1 (49%)	Obs2 (16%)	Obs3 (12%)	Obs4 (9%)
Mod1 (41%)	0.98	0.33	0.08	0.03
Mod2 (18%)	0.27	0.92	-0.14	0.13
Mod3 (9%)	-0.16	-0.16	0.27	0.87
Mod4 (9%)	0.04	-0.03	0.86	-0.35

(b) Spring (MAM).

	Obs1 (35%)	Obs2 (21%)	Obs3 (11%)	Obs4 (9%)
Mod1 (49%)	0.97	0.01	0.21	-0.02
Mod2 (13%)	0.30	0.42	0.36	0.33
Mod3 (7%)	0.11	-0.76	0.38	0.45
Mod4 (7%)	0.03	0.23	-0.61	0.66

(c) Summer (JJA).

	Obs1 (35%)	Obs2 (16%)	Obs3 (11%)	Obs4 (6%)
Mod1 (37%)	0.78	0.30	-0.35	-0.14
Mod2 (14%)	-0.37	-0.11	0.41	0.17
Mod3 (10%)	-0.34	0.07	-0.58	0.37
Mod4 (8%)	-0.11	0.64	-0.34	-0.49

(d) Autumn (SON).

	Obs1 (30%)	Obs2 (23%)	Obs3 (14%)	Obs4 (9%)
Mod1 (31%)	0.74	0.62	-0.16	-0.09
Mod2 (17%)	-0.43	0.76	-0.24	0.27
Mod3 (13%)	0.18	-0.15	0.88	0.08
Mod4 (10%)	0.38	-0.45	-0.44	0.60

Table 3 Number of years of above (first value) and below (second value) average observed NAO for each of 5 SST categories based on the amplitude of Atlantic SST EOF1 in the same season (see text for details). χ^2 values, and their associated significance, are also shown.

	DJF	JFM	FMA	MAM	AMJ
Category 1	5 : 4	7 : 2	9 : 0	8 : 1	8 : 1
Category 2	4 : 5	7 : 2	9 : 0	6 : 3	5 : 4
Category 3	7 : 2	5 : 4	3 : 6	4 : 5	2 : 7
Category 4	4 : 5	1 : 8	4 : 5	3 : 6	2 : 7
Category 5	4 : 5	1 : 8	2 : 7	4 : 5	5 : 4
χ^2 (%Sig)	3.2	16.6 (99)	21.9 (99.9)	7.7	11.2 (95)

Table 4 As table 3, but numbers of years of above and below average ensemble mean simulated NAO.

	DJF	JFM	FMA	MAM	AMJ
Category 1	5 : 4	6 : 3	8 : 1	6 : 3	7 : 2
Category 2	4 : 5	5 : 4	2 : 7	5 : 4	5 : 4
Category 3	8 : 1	6 : 3	6 : 3	4 : 5	3 : 6
Category 4	3 : 6	3 : 6	3 : 6	6 : 3	6 : 3
Category 5	5 : 4	3 : 6	4 : 5	3 : 6	3 : 6
χ^2 (%Sig)	6.8	4.1	10.3 (95)	3.2	5.9

FIG.1. MSLP 1961-90 seasonal climatologies. Observed data from the Basnett-Parker data set: (a) DJF, (b) MAM, (c) JJA, (d) SON. Ensemble mean of 6 model runs: (e) DJF, (f) MAM, (g) JJA, (h) SON. Units: hPa.

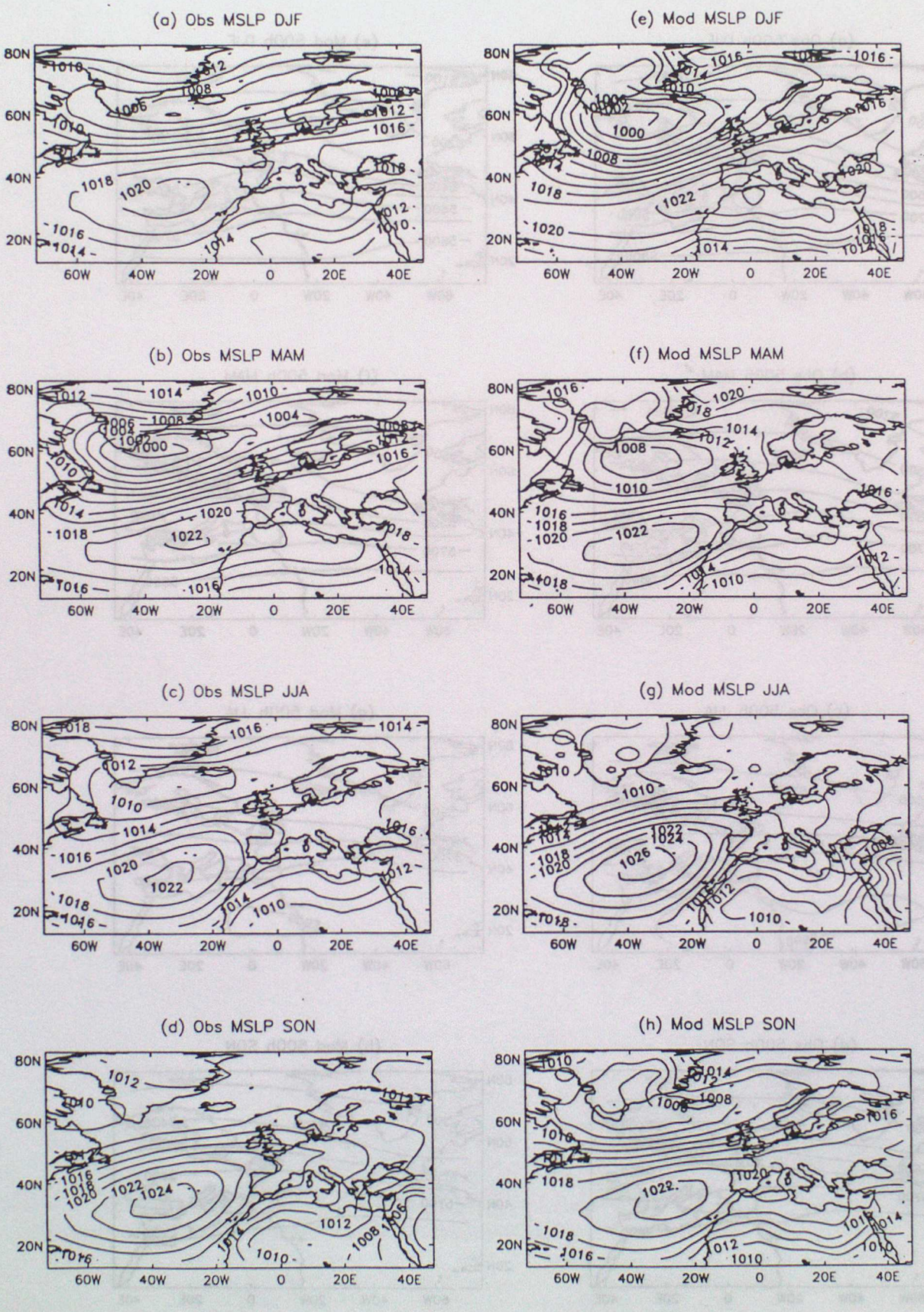

FIG.2. 500hPa height 1961-90 seasonal climatologies. Observed data from UK Met. Office operational archives: (a) DJF, (b) MAM, (c) JJA, (d) SON. Ensemble mean of 6 model runs: (e) DJF, (f) MAM, (g) JJA, (h) SON. Units: m.

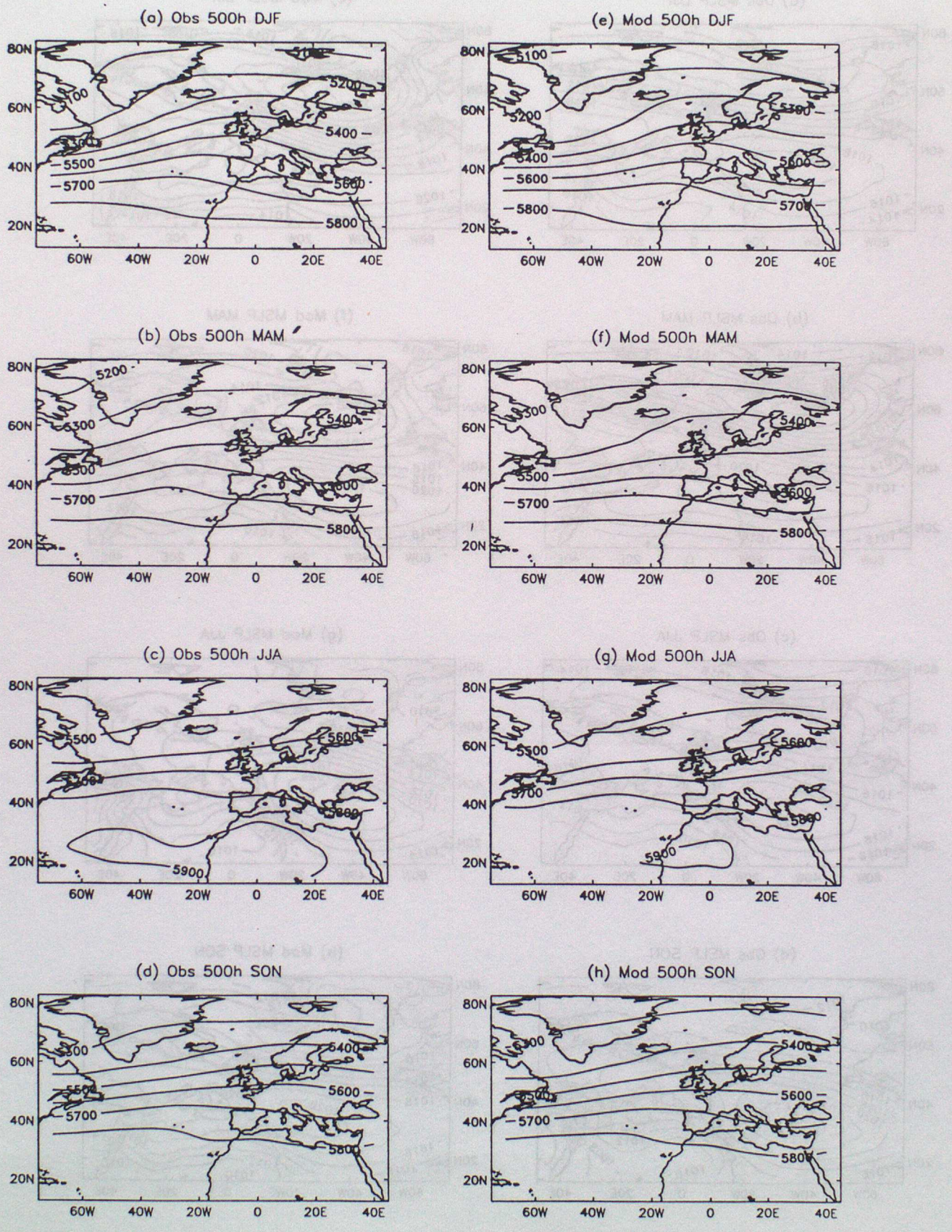

FIG.3. Unrotated covariance first EOF of seasonally averaged MSLP for 1949-93 over the area 20°N-80°N, 75°W-40°E calculated for an equal area grid of approximate resolution 500km latitude by 700km longitude. The percentage variance represented by each EOF is printed on each frame. Observed: (a) DJF, (b) MAM, (c) JJA, (d) SON. Modelled: (e) DJF, (f) MAM, (g) JJA, (h) SON. Units: point correlations with EOF time series. Negative loadings are indicated by dashed contours.

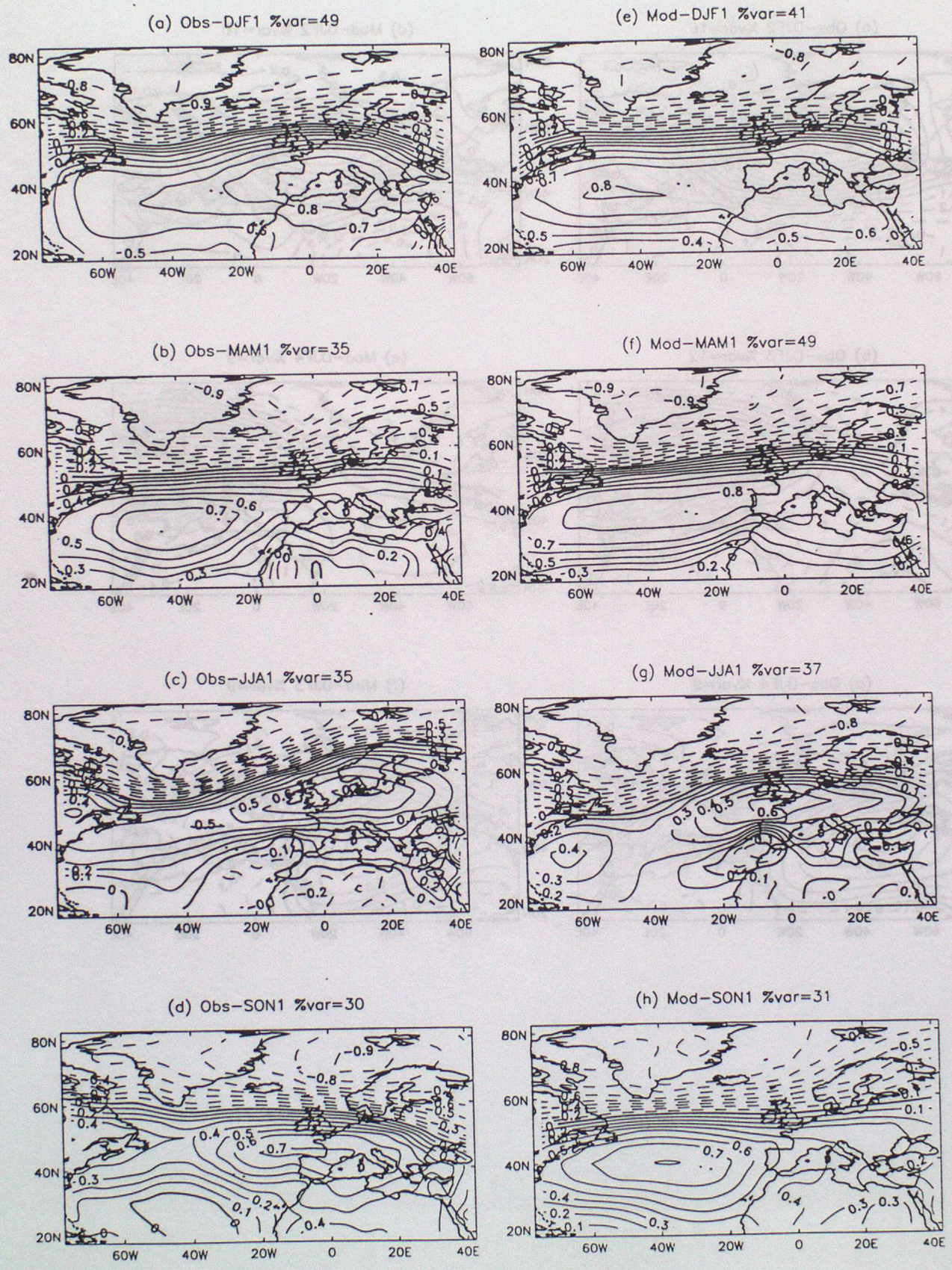

FIG.4. As fig.3, but lower order EOFs. Observed: (a) DJF EOF2, (b) DJF EOF3, (c) DJF EOF4. Modelled: (d) DJF EOF2, (e) DJF EOF4, (f) DJF EOF3.

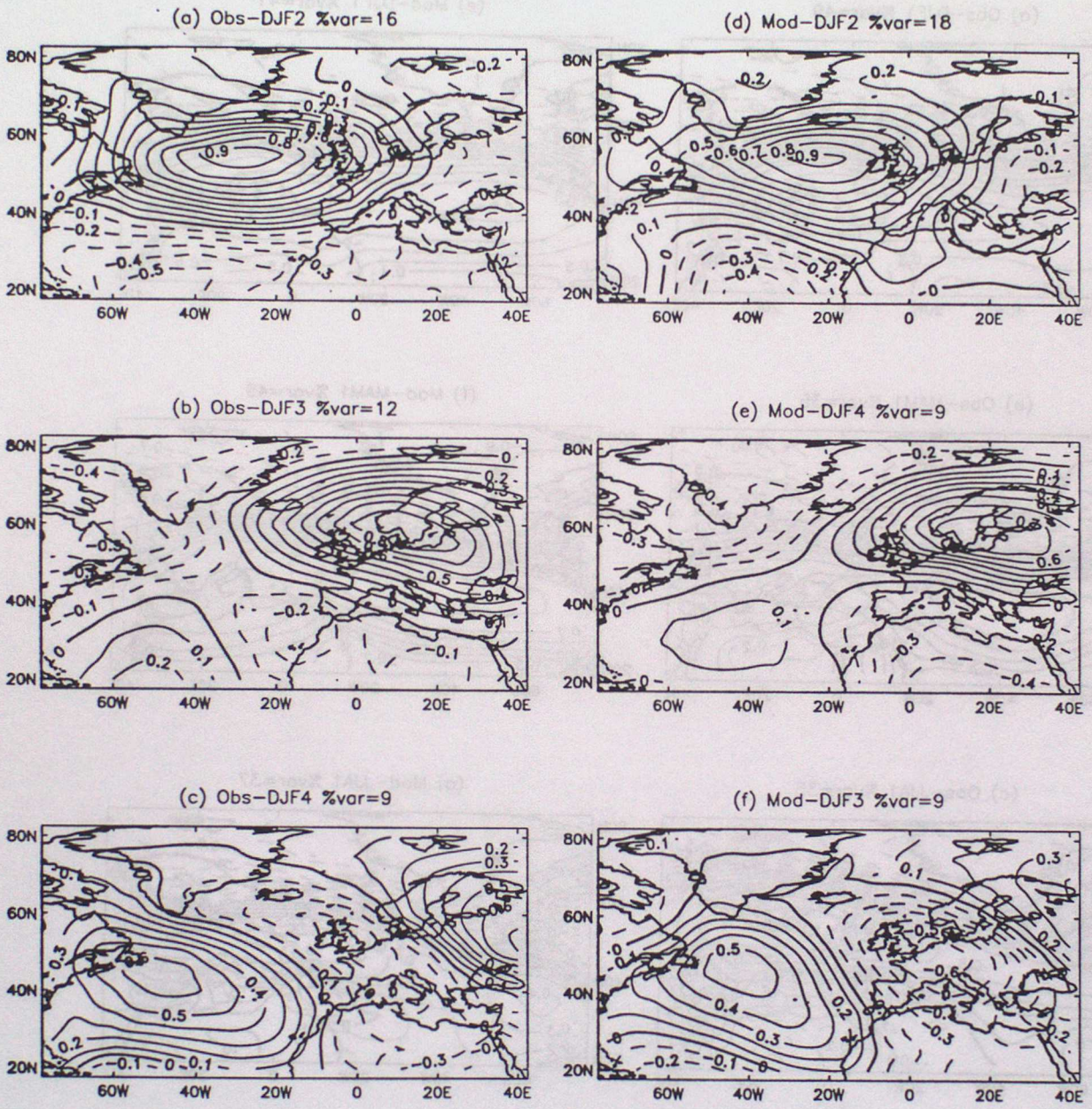

FIG.5. Observed (solid thick line) and model (solid thin line) westerly index (see text for details) for 3-month running mean calendar seasons. Also, observed (dashed thick line) and modelled (dashed thin line) interannual standard deviations of the westerly index. Values are plotted at the middle month of each season.

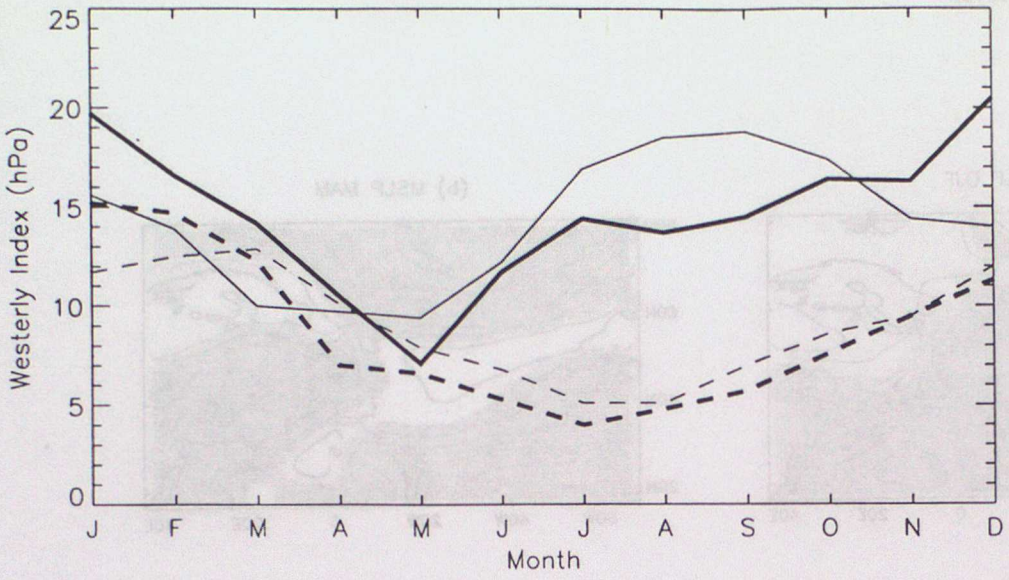

FIG.6. Percentage of total variance caused by SST and sea-ice forcing for seasonal MSLP during 1949-93. (a) DJF, (b) MAM, (c) JJA, (d) SON. Stippling indicates areas where values are significantly different from zero at the 95% level.

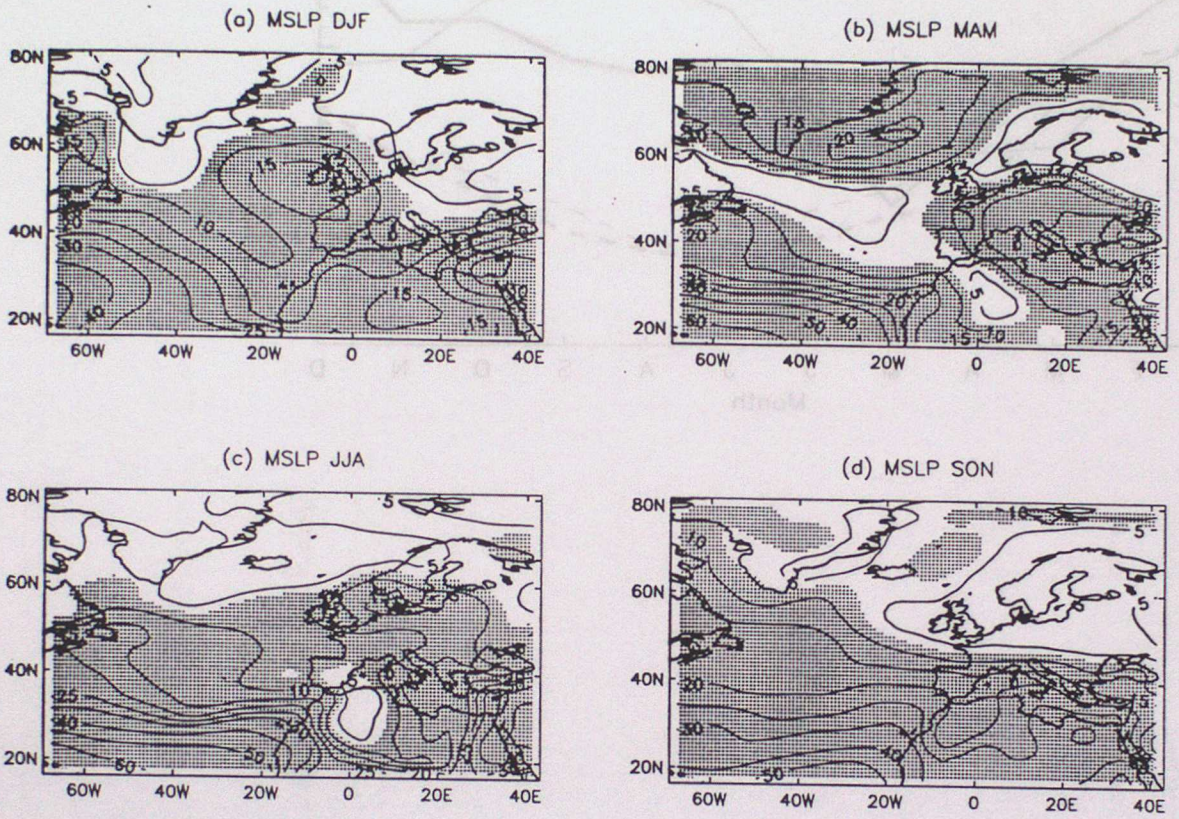

FIG.7. As fig.6 but seasonal 1.5m air temperature. Model land grid points are outlined, and values greater than 6% are significantly different from zero at the 95% level (no stippling is used).

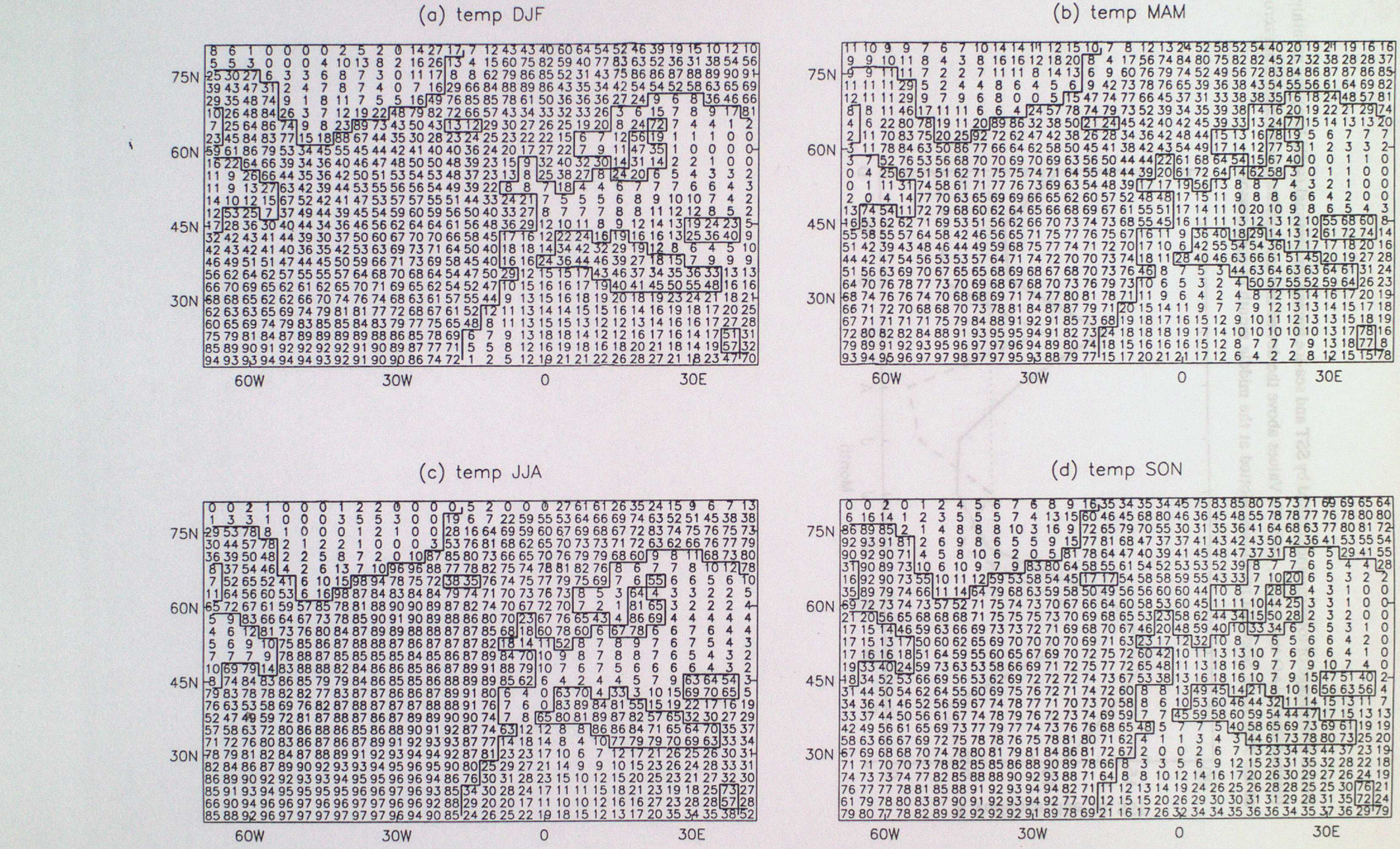

FIG.8. Percentage of total variance caused by SST and sea-ice forcing for seasonal (solid line) and monthly (dashed line) NAO time series, 1949-93. Values above the dotted line are significantly different from zero at the 95% level. Seasonal results are plotted at the middle month of each season.

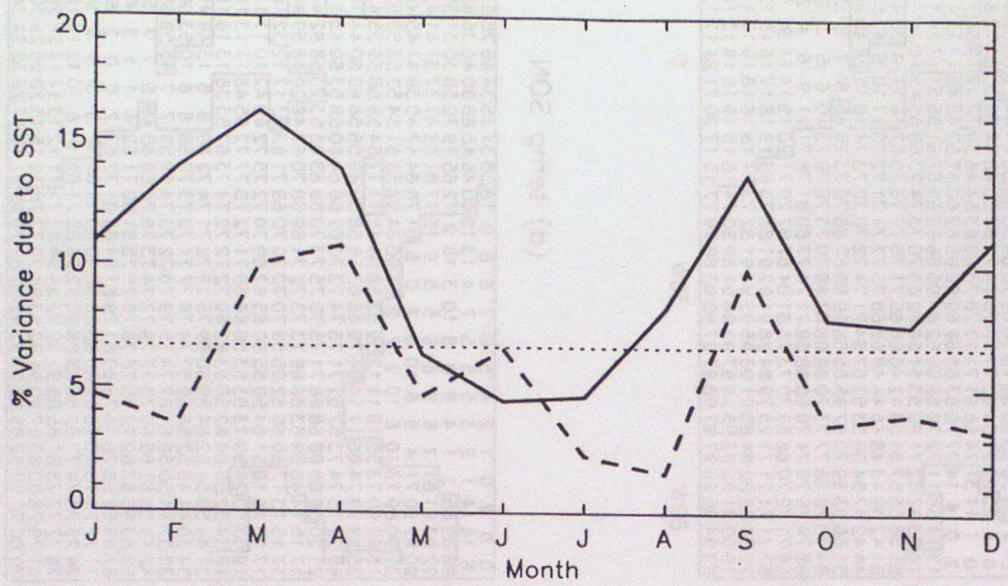

FIG.9. The correlation at each grid point between model ensemble mean seasonal MSLP data and observed data, for 1949-93. (a) DJF, (b) MAM, (c) JJA, (d) SON. Stippling indicates areas where values are significantly different from zero at the 95% level. Negative correlations are indicated by dashed contours.

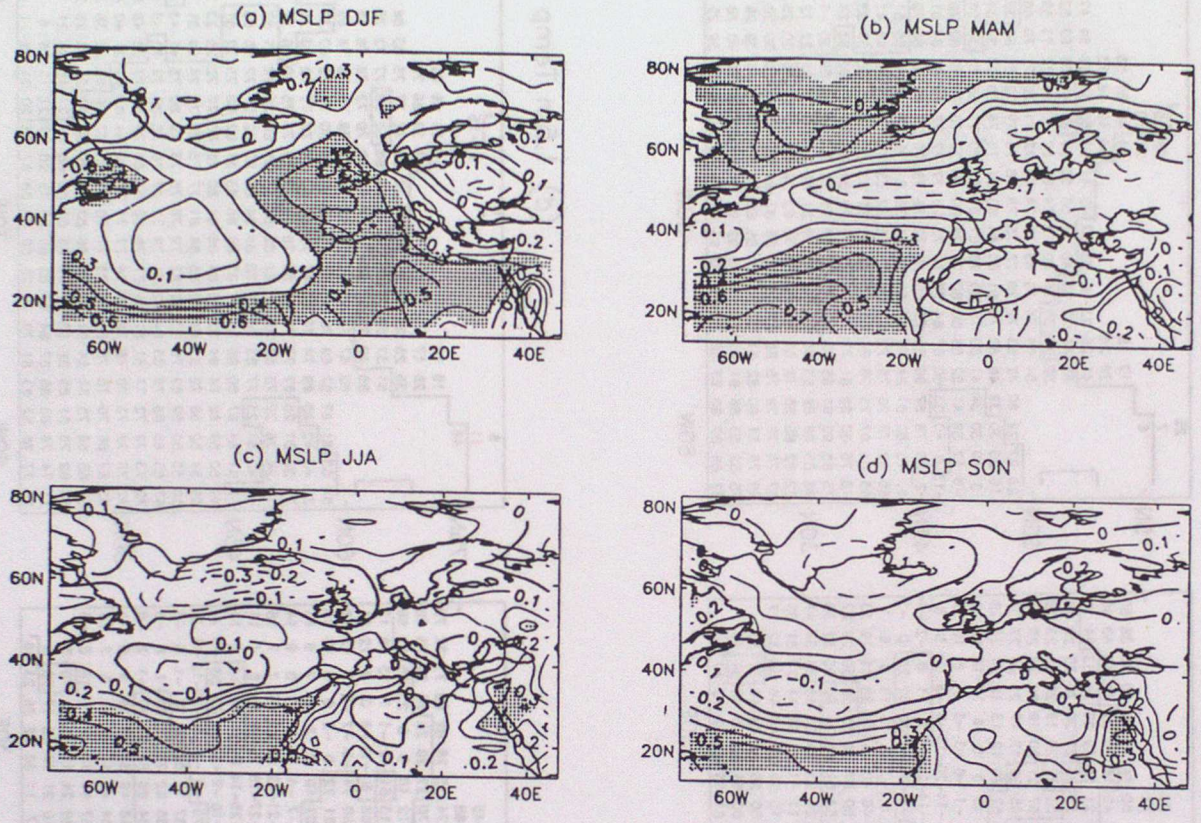

FIG.10. The correlation at each grid point between model ensemble mean seasonal 1.5m air temperature and observed air temperature, for 1949-93. (a) DJF, (b) MAM, (c) JJA, (d) SON. Model land grid points are outlined.

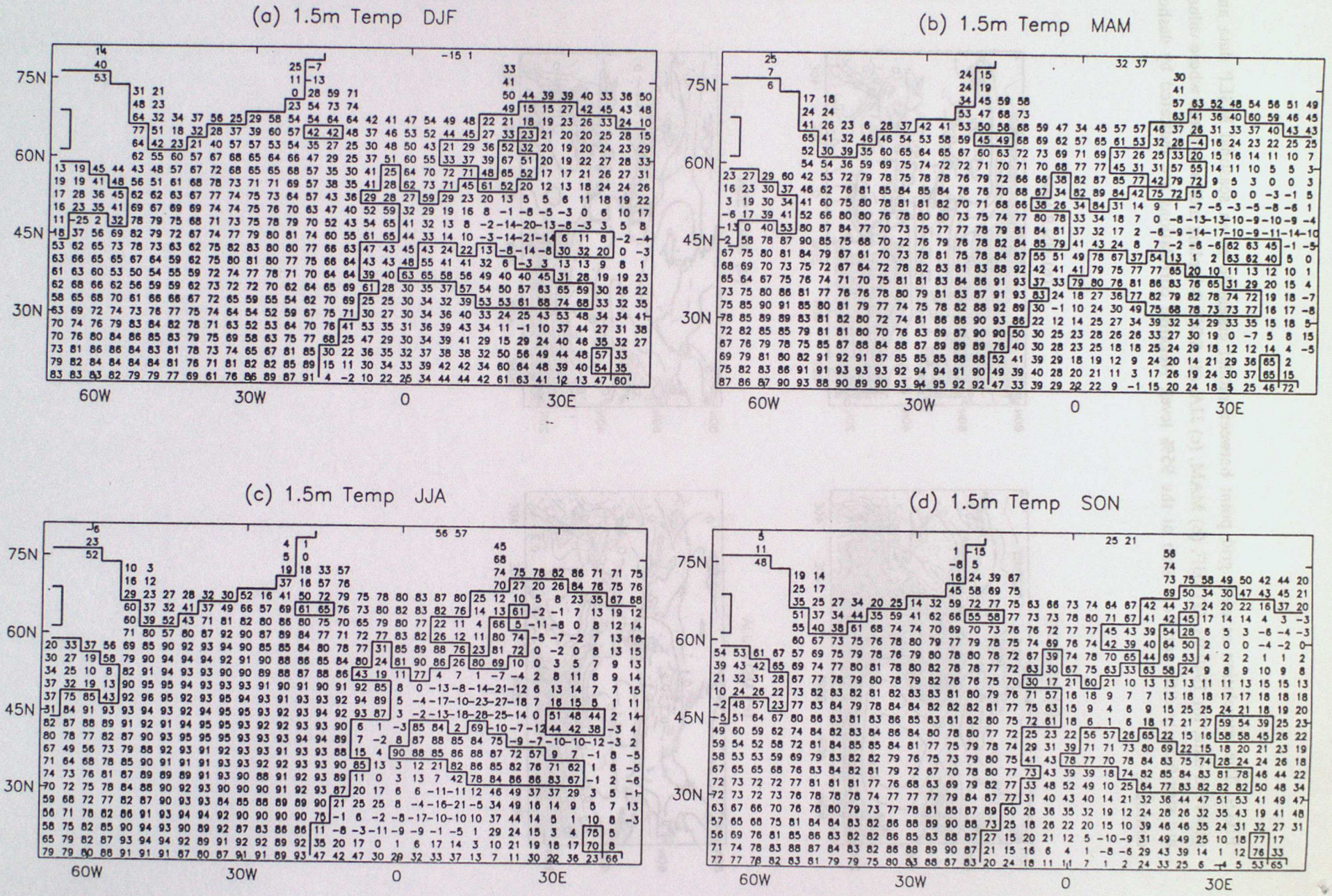

FIG.11. Correlation between observed NAO and model ensemble mean NAO calculated for 1949-93 with monthly data (dashed line) and seasonal data (solid line). Seasonal results are plotted at the middle month of each season. Correlations above the upper dotted line are significantly different from zero at the 95% level (neglecting autocorrelation, which is statistically insignificant for all the NAO time series).

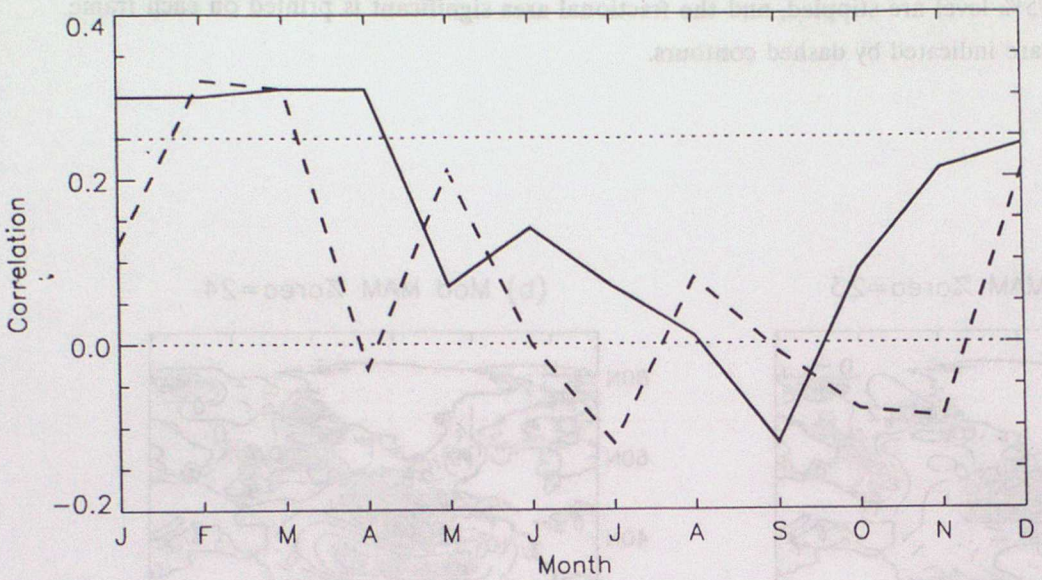

FIG.12. Composite difference of MAM high-frequency filtered SST, based on years of high NAO minus years of low NAO. (a) For observed NAO, (b) for modelled NAO. Areas where the composite difference is significant at the 95% level are stippled, and the fractional area significant is printed on each frame. Negative differences are indicated by dashed contours.

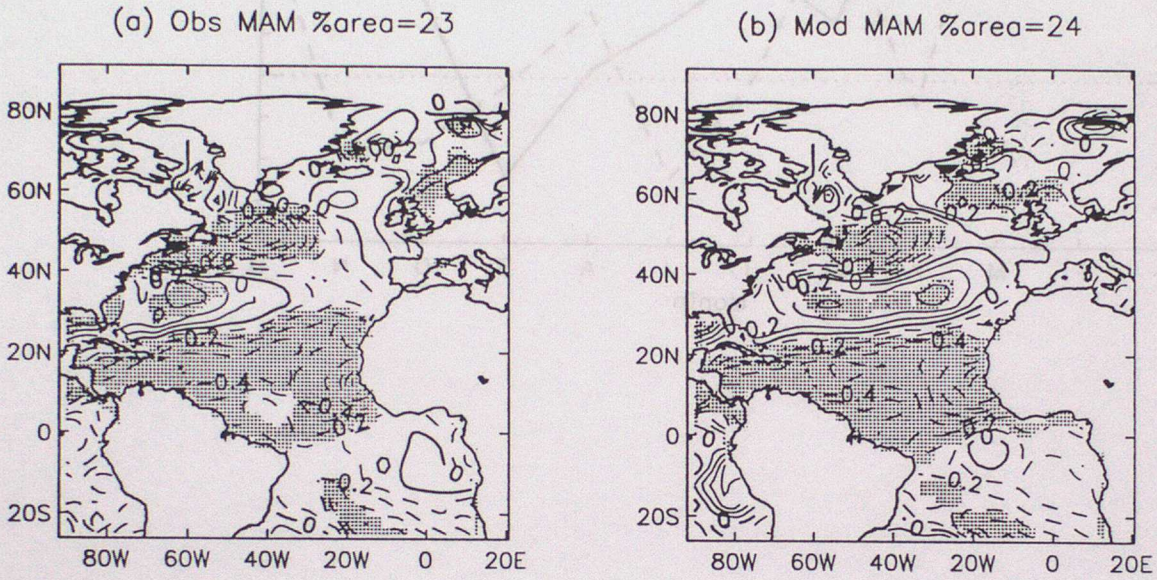

FIG.13. Composites of JFM high-frequency filtered observed and modelled 500hPa height for El Nino (warm) and La Nina (cold) years: (a) Observed composite anomaly (from 1961-90) for warm years, (b) observed composite anomaly for cold years, (c) observed composite difference for warm years minus cold years, (d)-(f) as (a)-(c) but model data. Areas where the composites are significant at the 95% level are stippled, and the fractional area significant is printed on each frame. Negative values are indicated by dashed contours. Thin boxed areas surround missing observed data.

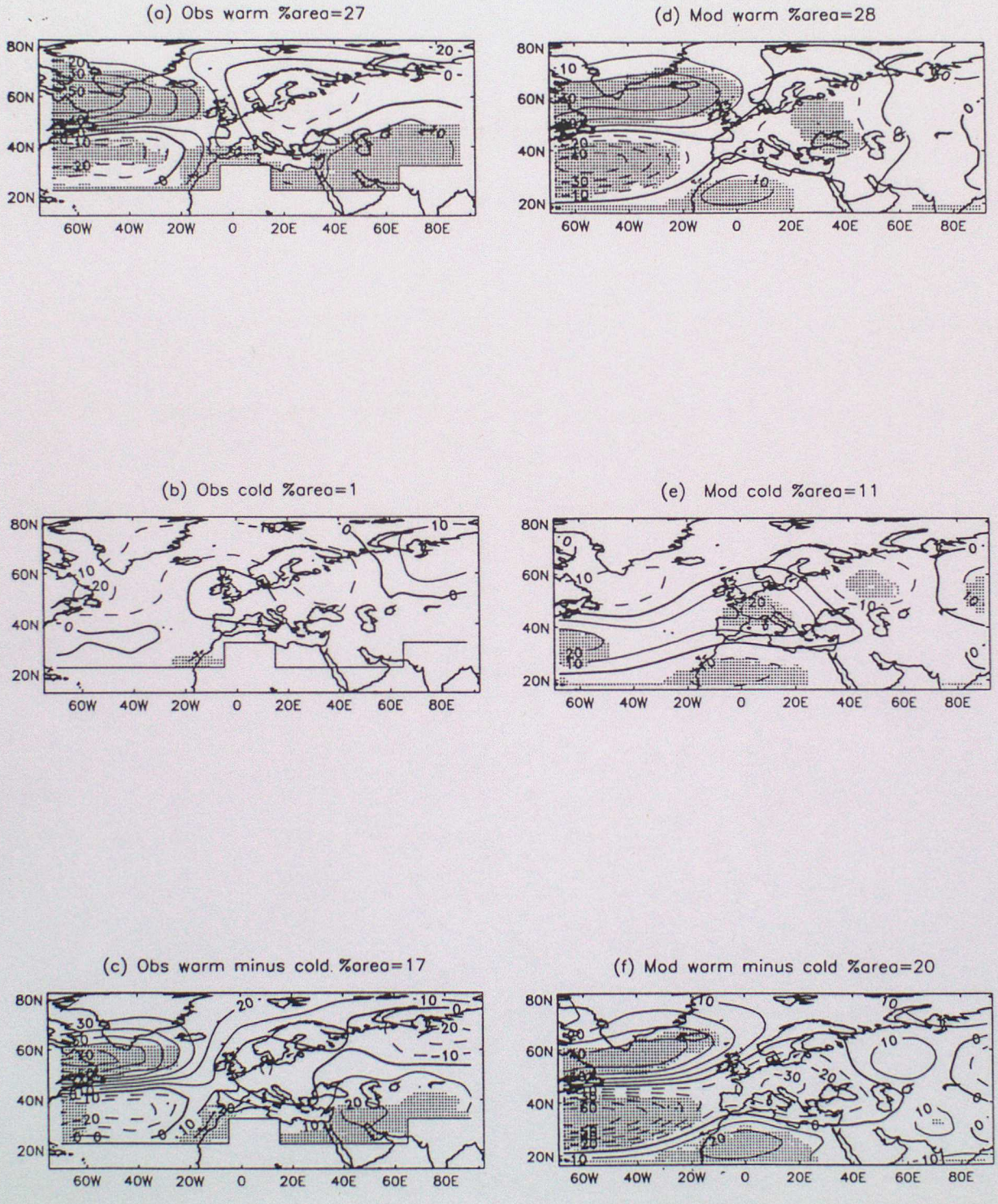

CLIMATE RESEARCH TECHNICAL NOTES

CRTN 1	Oct 1990	Estimates of the sensitivity of climate to vegetation changes using the Penman-Monteith equation. P R Rowntree
CRTN 2	Oct 1990	An ocean general circulation model of the Indian Ocean for hindcasting studies. D J Carrington
CRTN 3	Oct 1990	Simulation of the tropical diurnal cycle in a climate model. D P Rowell
CRTN 4	Oct 1990	Low frequency variability of the oceans. C K Folland, A Colman, D E Parker and A Bevan
CRTN 5	Dec 1990	A comparison of 11-level General Circulation Model Simulations with observations in the East Sahel. K Maskell
CRTN 6	Dec 1990	Climate Change Prediction. J F B Mitchell and Qing-cun Zeng
CRTN 7	Jan 1991	Deforestation of Amazonia - modelling the effects of albedo change. M F Mylne and P R Rowntree
CRTN 8	Jan 1991	The role of observations in climate prediction and research. D J Carson
CRTN 9	Mar 1991	The greenhouse effect and its likely consequences for climate change. D J Carson
CRTN 10	Apr 1991	Use of wind stresses from operational N.W.P. models to force an O.G.C.M. of the Indian Ocean. D J Carrington
CRTN 11	Jun 1991	A new daily Central England Temperature series, 1772-1991. D E Parker, T P Legg and C K Folland
CRTN 12	Jul 1991	Causes and predictability of Sahel rainfall variability. D P Rowell, C K Folland, K Maskell, J A Owen, M N Ward

CLIMATE RESEARCH TECHNICAL NOTES

CRTN 13	Jul 1991	Modelling changes in climate due to enhanced CO2, the role of atmospheric dynamics, cloud and moisture. C A Senior, J F B Mitchell, H Le Treut and Z-X Li
CRTN 14	Sep 1991	Sea temperature bucket models used to correct historical SST data in the Meteorological Office. C K Folland
CRTN 15	Aug 1991	Modelling climate change, and some potential effects on agriculture in the U.K. P R Rowntree, B A Callander and J Cochrane
CRTN 16	Aug 1991	The Boreal Forests and Climate G Thomas and P R Rowntree
CRTN 17	Aug 1991	Development of a Stratosphere-Troposphere Data Assimilation System. R Swinbank.
CRTN 18	Sep 1991	A study of asynchronous coupling using a simple climate model. M K Davey.
CRTN 19	Sep 1991	The Oceanic Carbon Cycle. N K Taylor
CRTN 20	Nov 1991	Worldwide ocean-atmosphere surface fields in Sahel wet and dry years using provisionally corrected surface wind data. M N Ward
CRTN 21	Dec 1991	Coupled tropical ocean global atmosphere models at the UKMO. M K Davey, C Gordon, S Ineson and S Lawrence
CRTN 22	Dec 1991	Empirical parameterisation of tropical ocean-atmosphere coupling. M Allen, M K Davey, D L T Anderson and P D Killworth
CRTN 23	Feb 1992	The temporal evolution of Equatorial Currents in the Indian Ocean D L T Anderson, D J Carrington, R A Corry and C Gordon
CRTN 24	Feb 1992	Stratospheric analyses provided by the U.K. Meteorological Office M J Bailey, A O'Neill and V D Pope

CLIMATE RESEARCH TECHNICAL NOTES

CRTN 25	Feb 1992	Modelling interannual variability in the Indian Ocean using momentum fluxes from the UKMO and ECMWF operational weather analyses. D L T Anderson and D J Carrington
CRTN 26	Mar 1992	A GCM simulation of the impact of Amazonian deforestation on climate using an improved canopy representation J Lean and P R Rowntree
CRTN 27	Mar 1992	The parameterization of rainfall interception in GCMs A J Dolman and D Gregory
CRTN 28	Jun 1992	Development of worldwide marine data eigenvectors since 1985 A W Colman
CRTN 29	Jun 1992	A tropical ocean model with reduced physics M K Davey
CRTN 30	Jun 1992	International Temperature Workshop, Boulder, Colorado, USA, 16 January 1992 Edited by D E Parker
CRTN 31	Jul 1992	Simulation of clear-sky outgoing longwave radiation over the oceans using operational analyses A Slingo and M J Webb
CRTN 32	Sep 1992	A prediction of the transient response of climate J M Murphy
CRTN 33	Nov 1992	LEPS scores for assessing climate model simulations and long-range forecasts. C K Folland
CRTN 34	Jan 1993	Stratospheric Data Assimilation System Guide Editer: R Swinbank
CRTN 35	Mar 1993	A Stratosphere-Troposphere Data Assimilation System R Swinbank and A O'Neill
CRTN 36	Mar 1993	Validation of hydrological schemes for climate models against catchment data. P R Rowntree and J Lean

CLIMATE RESEARCH TECHNICAL NOTES

CRTN 37 Apr 1993 Modelling of palaeoclimates: Examples from the recent past
J F B Mitchell

CRTN 38 May 1993 A simulation of seasonality in ENSO forecast skill
M K Davey, D L T Anderson and S Lawrence

CRTN 39 Jul 1993 ENSO Prediction experiments using a simple ocean-atmosphere model
D-H Wu, D L T Anderson and M K Davey

CRTN 40 Sep 1993 Diagnosis of dynamic sea-surface and sea-level changes from the Cox ocean model
J M Gregory

CRTN 41 Sep 1993 Seasonal variations of the clear-sky greenhouse effect: the role of changes in atmospheric temperatures and humidities
M J Webb, A Slingo and G L Stephens

CRTN 42 Nov 1993 Sea-level changes under increasing atmospheric CO_2 in a transient coupled ocean-atmosphere GCM experiment.
J M Gregory

CRTN 43 Dec 1993 Global and regional patterns of climate change: recent predictions for the Arctic
P R Rowntree

CRTN 44 Feb 1994 The effect of changing horizontal diffusion in the atmospheric version of the unified climate model
C D Hall and R A Stratton

CRTN 45 Mar 1994 Simulation of El-Niño/Southern Oscillation like variability in a global AOGCM and its response to CO_2 increase.
S F B Tett

CRTN 46 Apr 1994 Global data required for monitoring climate change.
D E Parker and C K Folland

CRTN 47 May 1994 Seasonal uptake of anthropogenic CO_2 in an ocean general circulation model.
N K Taylor

CLIMATE RESEARCH TECHNICAL NOTES

CRTN 48	Jun 1994	A tropic-wide oscillation of boreal summer rainfall and patterns of sea-surface temperature. M N Ward, K Maskell, C K Folland, D P Rowell and R Washington
CRTN 49	Jun 1994	Simulation of the tropical Pacific using a simplified ocean model M A Balmaseda, D L T Anderson and M K Davey
CRTN 50	Sep 1994	Simulation of global mean temperature using a box-diffusion climate model P R Rowntree
CRTN 51	Sep 1994	Seasonal dependence of ENSO prediction skill M A Balmaseda, M K Davey and D L T Anderson
CRTN 52	Nov 1994	Simulation of the Indian Monsoon and Tropical Intraseasonal Variability by a General Circulation Model P M Inness and D Gregory
CRTN 53	Mar 1995	A comparison of modelled surface fluxes with climatological estimates. C Gordon and D K Wright
CRTN 54	Mar 1995	The representation of moist convection in atmospheric models. D Gregory
CRTN 55	Mar 1995	A consistent treatment of the evaporation of rain and snow for use in large-scale models D Gregory
CRTN 56	Apr 1995	Workshop on simulations of the Climate of the Twentieth Century using GISST, 28-30 November 1994, Hadley Centre, Bracknell, UK Edited by C K Folland and D P Rowell
CRTN 57	May 1995	Enhanced shortwave cloud radiative forcing due to anthropogenic aerosols. S E Swartz and A Slingo
CRTN 58	May 1995	The simulation of the tropical oceans in models of different horizontal resolution. C Gordon, D K Wright and C M Roberts
CRTN 59	Sep 1995	The water budget of middle latitude continental regions - a modelling and observational study P R Rowntree
CRTN 60	Sep 1995	Intraseasonal variability of the Indian summer monsoon simulated by the Hadley Centre climate model K Ashok, D Gregory and P M Inness

CLIMATE RESEARCH TECHNICAL NOTES

CRTN 61	Sep 1995	Climate simulations with the Unified Model: AMIP runs C D Hall, R A Stratton and M L Gallani
CRTN 62	Nov 1995	Validation of surface parameters over the oceans in climate simulations with the unified model. C D Hall
CRTN 63	Dec 1995	The GISST2.2 sea surface temperature and sea-ice climatology D E Parker, M Jackson and E B Horton
CRTN 64	Dec 1995	Parametrization of momentum transport by convection. II: Tests in single column and general circulation models. D Gregory, R Kershaw and P M Inness
CRTN 65	Jan 1996	Understanding the sensitivity of a GCM simulation of Amazonian deforestation to the specification of vegetation and soil characteristics. J Lean and P R Rowntree
CRTN 66	Jan 1996	On the efficient calculation of infra-red fluxes and cooling rates using the two-stream equations. J M Edwards
CRTN 67	Jan 1996	The second Hadley Centre coupled ocean-atmosphere GCM: Model description, spinup and validation. TC Johns,RE Carnell,JF Crossley,JM Gregory, JFB Mitchell,CA Senior,SFB Tett and RA Wood
CRTN 68	Feb 1996	The sensitivity of climate simulations to the specification of mixed phase clouds D Gregory and D Morris
CRTN 69	Apr 1996	Using an ensemble of Multi-Decadal GCM simulations ro assess potential seasonal predictability D P Rowell
CRTN 70	May 1996	North Atlantic and European Seasonal Predictability using an Ensemble of Multi-Decadal AGCM Simulations J R Davies, D P Rowell and C K Folland